

# Uniform cell seeding and generation of overlapping gradient profiles in a multiplexed microchamber device with normally-closed valves

**Bobak Mosadegh,<sup>a</sup> Mayank Agarwal,<sup>a</sup> Hossein Tavana,<sup>a</sup> Tommaso Bersano-Begey,<sup>a</sup> Yu-suke Torisawa,<sup>a</sup> Maria Morell,<sup>c</sup> Matthew J. Wyatt,<sup>c</sup> K. Sue O'Shea,<sup>c</sup> Kate F. Barald<sup>ac</sup> and Shuichi Takayama <sup>\*abd</sup>**

Received 9th June 2010, Accepted 17th August 2010

DOI: 10.1039/c0lc00086h

Generation of stable soluble-factor gradients in microfluidic devices enables studies of various cellular events such as chemotaxis and differentiation. However, many gradient devices directly expose cells to constant fluid flow and that can induce undesired responses from cells due to shear stress and/or wash out of cell-secreted molecules. Although there have been devices with flow-free gradients, they typically generate only a single condition and/or have a decaying gradient profile that does not accommodate long-term experiments. Here we describe a microdevice that generates several chemical gradient conditions on a single platform in flow-free microchambers which facilitates steady-state gradient profiles. The device contains embedded normally-closed valves that enable fast and uniform seeding of cells to all microchambers simultaneously. A network of microchannels distributes desired solutions from easy-access open reservoirs to a single output port, enabling a simple setup for inducing flow in the device. Embedded porous filters, sandwiched between the microchannel networks and cell microchambers, enable diffusion of biomolecules but inhibit any bulk flow over the cells.

## Introduction

Over the past decade, microfluidic devices have been used to create controlled microenvironments for cell studies.<sup>1</sup> In particular, generation of stable concentration gradients is one unique advantage of microfluidic devices over macro-scale systems.<sup>2</sup> Due to the importance of soluble-factor gradients in cell biological contexts, many gradient-generating devices have been used to study a variety of cellular events such as chemotaxis<sup>3–5</sup> and differentiation.<sup>6–8</sup> The first microfluidic gradient devices generated spatially-controlled concentration profiles facilitated by free diffusion of reagents across laminar flows of varying reagent concentrations.<sup>4,9,10</sup> Although these devices have provided valuable insights into many gradient-mediated processes, direct fluid flow on cells imposes shear stress effects and washes out autocrine factors. This can adversely affect cellular behavior and confound experimental data.<sup>5,11</sup> To overcome these limitations, static gradient devices have been developed that eliminate fluid shear stress and generate gradients primarily through diffusion.<sup>12–15</sup> In these static devices, retention of autocrine factors can permit vital physiological processes to occur under more *in vivo*-like microenvironmental conditions.<sup>2</sup> Static gradients are typically generated in a chamber or channel that is connected to a source solution (containing a desired concentration of the biomolecule of interest) and a sink solution (having a lower concentration of the desired biomolecule) at its two ends.<sup>12–14,16</sup> Bulk flow in the chamber or channel is negated

by high resistance created by small channel features,<sup>12,16–18</sup> small-pore membranes,<sup>13,19,20</sup> or dense hydrogels.<sup>12,16,21,22</sup> Gradients can be made to be either stable or transient with respect to time using a continuously replenishing<sup>12,16–20,22</sup> or a finite volume<sup>13,21</sup> of the source and sink solutions, respectively. Although the finite volume approach is more practical and does not require continuous flow, it is not ideal for long term studies (more than a few hours) due to the time-decay of the gradient. Stable static gradient devices use continuous infusion of solutions by a multi-syringe pump, which is cumbersome and requires significant dead volumes of solutions, which can be expensive, and yet accommodate only one test condition.

To address the above issues, we have developed a microfluidic gradient device with embedded filters to simultaneously generate multiple static microenvironments with steady-state gradient profiles. The chambers are separated by integrated normally-closed valves (valves that are in a closed position when not pressurized)<sup>23</sup> that allow easy and uniform seeding of cells in all chambers. The embedded filters enable diffusion of soluble factors while negating bulk flow through the cell chambers. The device only requires the user to pipette desired solutions into three reservoirs and induce flow through one outlet tube. Using this device, we demonstrate that a population of cells take up a stain according to their relative position in a gradient of three different types of media. This approach can provide parallel, user-friendly, testing capabilities and the device can serve as a valuable platform to investigate cellular behavior in controlled static microenvironments.

## Experimental

### Device fabrication

The device consists of four layers, each made from PDMS prepolymer and curing agent (Sylgard 184, Dow Corning Co.,

<sup>a</sup>Department of Biomedical Engineering, University of Michigan, Ann Arbor, 48109. E-mail: takayama@umich.edu

<sup>b</sup>Macromolecular Science and Engineering Center, University of Michigan, Ann Arbor, 48109

<sup>c</sup>Department of Cell and Developmental Biology, University of Michigan, Ann Arbor, 48109

<sup>d</sup>Division of Nano-Bio and Chemical Engineering WCU Project, UNIST, Ulsan, Republic of Korea

Midland, MI) at a 10 : 1 ratio. The top and bottom thick layers are cast against a master mold fabricated by standard photolithography using the negative-photoresist SU-8 2025 (SU-8, Micro-Chem Co., Newton, MA). The height of the features in both the top layer and bottom layer are 80  $\mu\text{m}$ . The master molds are silanized with tridecafluoro-1,1,2,2-tetrahydrooctyl trichlorosilane (United Chemical Tech., Bristol, PA) in a desiccator for 2 h to minimize bonding between PDMS and the master mold.<sup>24</sup> The PDMS molds of the top and bottom layers are cured in a 120 °C oven for 2 h. All layers are bound together after oxygen plasma treatment (SPI Plasma-Prep II, Structure Probe, Inc., West Chester, PA) for 30 s. The filters used are punched out with a 2 mm diameter biopsy punch from a 200 nm pore-size polycarbonate filter (Cat.# 7060-4702, Whatman, Piscataway, NJ).

The two PDMS membranes (20  $\mu\text{m}$  thickness) are made by spin coating on silanized glass slides at 3000 rpm for 60 s and then curing in a 120 °C oven for 30 min. The top and bottom thick layers are then bound to each membrane while still on their glass slides. For the bottom layer, a PDMS stamp that has extruding features that match the locations of the normally-closed valves is put into contact with the bottom layer. This step transfers free PDMS oligomers to the bottom layer, which acts as a passivation layer, and negates bonding of the membrane to the valve regions when subsequently bonded by plasma oxidation. After bonding, the two composite layers can be removed easily by simply peeling the device off the glass slide. Holes are then manually punched into the membranes using a 0.35 mm dermal biopsy punch (Prod# 15070, Harris Uni-Core, Ted Pella) at specified locations where a fluid needs to pass between the top and bottom layers of the device. A scalpel and tweezers are used to cut out regions of the membrane that block the bottom layer from its access holes (*i.e.* vacuum port, cell inlet and outlet) and the regions where the filters will be located (that are 500  $\mu\text{m}$  wide and 1.5 mm long). These manual operations are done under a stereoscope (Nikon SMZ600). The filters are then placed on the bottom layer at the designated locations and the two composite layers are treated with oxygen plasma for 30 s. Since the filters can be placed on the bottom layer before the plasma treatment, repositioning of the filters in their correct locations is not hindered. The two composite layers are then manually aligned and bound under a stereoscope and the force from the bound layers maintains the filters in position. In addition, having the two membrane layers on each side of the filters ensures that there is proper sealing around the entire circumference of the filter even where there are channel features.

### Cell culture

Mouse ES cells (D3 mESC cell line; ATCC) are cultured in medium containing DMEM supplemented with 15% v/v knockout serum replacement (KSR), 0.1 mM 2-mercaptoethanol, 0.02% v/v sodium pyruvate, 1% v/v non-essential amino acids, 100 U mL<sup>-1</sup> penicillin, 100 U mL<sup>-1</sup> streptomycin, and 2000 U mL<sup>-1</sup> ESGRO, which contains leukemia inhibitory factor (LIF), in a humidified incubator maintained at 37 °C and 5% CO<sub>2</sub>. D3 mESC were transfected with an OCT4-EGFP plasmid using lipofectamine plus reagent (Invitrogen), a gift of Dr T. Gratsch, which was described previously.<sup>25</sup> Breast cancer cells (MDA-MB-231, ATCC) were cultured in medium

containing DMEM supplemented with 10% fetal bovine serum (FBS) and kept in a humidified incubator maintained at 37 degrees Celsius and 5% CO<sub>2</sub>.

### Simulation and experimental data

The cell culture chamber is 1cm wide and 500  $\mu\text{m}$  in height. The two overlapping regions with the filters are 1.5 mm wide and 500  $\mu\text{m}$  in height and their center is located 2.25 mm from the center of the cell culture chamber. The valves are not simulated, but the lengths of the cavity region and gap region are 1mm and 0.5 mm, respectively, and both features have a width of 0.5 mm. For purposes of the simulation (Comsol 3.4), the governing equations were based on pure diffusion and the boundary conditions were all insulated except for the two overlapping regions which were set to have a mass transfer coefficient of 1–10<sup>-6</sup> m/s and a bulk concentration of either 1 or 0. For the experimental data, solution reservoirs were filled with either green fluorescein or a buffer and withdrawn at a flowrate of 0.1  $\mu\text{l}/\text{min}$ . For the individual fluid channels, which are 300  $\mu\text{m}$  wide everywhere except over the filters where they are 500  $\mu\text{m}$  and 100  $\mu\text{m}$  at the solution reservoirs, their flowrate is approximately 16.67 nL/min. The device was allowed to reach steady-state and then images were taken using a fluorescence microscope. To approximate the time it takes to reach steady state, the following equation can be used,  $t = x^2/(2D)$ , where  $t$  is time,  $x$  is the distance between the two source and sink, and  $D$  is the diffusion coefficient. Calculating for the given microchamber used (which has an  $x$  value of 0.4 mm) and fluorescein solution which has a molecular weight of 332.31 Da ( $D \sim 4.5 \cdot 10^{-6} \text{ cm}^2/\text{s}$ ), the approximate time to steady-state is 2.78 h. Shortening the length between the source and sink fluid channel will exponentially decrease the time to achieve steady-state profiles.

### Cell seeding experiment

After construction of the device, fluids should be introduced into the device, after a 5 min plasma treatment, by filling the solution reservoirs and cell inlet and then applying a vacuum to the outlet and cell outlet using a micropipette. For this experiment, the device was filled with a 100  $\mu\text{g}/\text{ml}$  fibronectin solution. After 3 h, mESCs were seeded in the cell inlet port of the device using a micropipette. A volume of 10  $\mu\text{l}$  at  $4.5 \times 10^6 \text{ cell/ml}$  was deposited in the cell inlet and then the normally-closed valves were opened by applying a vacuum using a syringe connected by tubing to the vacuum port. The device was then tilted at 45 degrees to induce flow of the cell suspension through the device. After approximately 10 s, the syringe was released to close the valves. The device was then incubated at 37 °C for three hours in an incubator to allow cell attachment. Phase images of each microchamber were taken using an optical microscope (Nikon TE300) and then cells were counted using NIH ImageJ software. This process was repeated for three separate devices using the same cell suspension.

### Cell-staining gradient experiment

For this experiment, the device was filled with a 100  $\mu\text{g}/\text{ml}$  fibronectin solution. After 3 h, breast cancer cells (MDA-MB-231) were seeded in the device at  $1 \times 10^7 \text{ cells/ml}$ . All three solutions used for the solution reservoirs of the device had a base

medium of DMEM + 10% FBS (Invitrogen), one was supplemented with cell tracker green and another with cell tracker red (Invitrogen). 100  $\mu$ l of each medium was simultaneously added to their respective solution reservoirs using a multi-pipette. The three media were pumped through the device using a syringe pump at a withdrawal rate of 0.1  $\mu$ l/min for 24 h. The syringe was filled with dPBS and connected to a tube that was inserted into the outlet hole of the device. The tube was split by a three-way valve that could be manually turned on and off to ensure that no flow was induced when placing the syringe on the syringe pump.

## Results and discussion

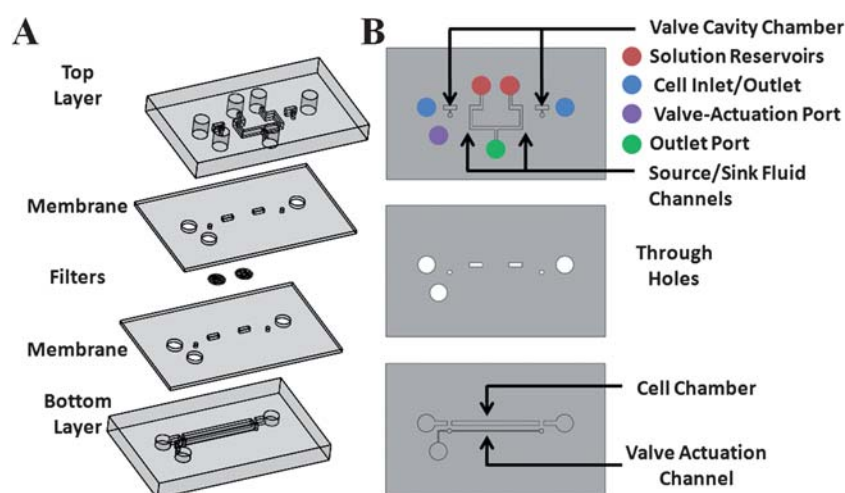
The gradient microchamber generates a gradient by passive diffusion of molecules from a source channel to a sink channel (both located in the top layer of the device) that is continually perfused to maintain a constant concentration profile (Fig. 1). The device consists of four PDMS layers: two thick molded layers and two thin membranes (Fig. 1A). The top and bottom layers contain 3D fluidic channel networks that distribute desired solutions to a cell chamber in the bottom layer. The PDMS membranes are punched with through-holes to connect the top and bottom channel networks (Fig. 1B). Embedded filters are placed to allow for the diffusion of molecules between the static cell chamber and flowing channel networks. Normally-closed valves are made by having a gap region and a cavity feature in the bottom and top layers, respectively, such that when a negative pressure is applied to the vacuum port, the PDMS membrane deflects into the cavity feature allowing fluid to bypass the gap region.<sup>14</sup>

Fig. 2 provides both the experimental data and simulation results of gradient profiles in the microchambers. The concentration profile depends on the concentration of molecules of interest in the solution loaded into fluidic channels (Fig. 2A). If the concentrations are equal in both fluid channels, a uniform steady-state profile will develop; otherwise the steady-state profile will be a linear gradient. This is shown by fluorescence intensity measurements of a fluorescein dye (Fig. 2B). These

profiles can only occur in the microchambers when there is no flow through the filters so that the only form of transport is diffusion of molecules as simulated in the finite element model (Fig. 2C, D).

An important consideration for gradient devices is that the material used for device fabrication should be cell-friendly and the design should allow for surface treatments that allow cells to adhere and grow in the device. For cell culture studies, the normally-closed valves in the microchamber can be opened to first introduce solutions containing extracellular matrix proteins (Fig. 3A, B). Subsequently, cells are flowed through and then valves are closed allowing cells to attach (Fig. 3C, D). Typically, uniform cell seeding in a microfluidic device is not trivial due to residual flow that causes higher cell density in upstream regions of the channel.<sup>26</sup> However, embedded valves in our microfluidic device overcome this existing limitation. A cell suspension is simply pipetted into the inlet and the device is tilted to allow gravity to induce the flow of cells toward the outlet. When the valves are closed, the flow instantly stops and cells become immobile and attach to the channel surface. This approach is advantageous compared to existing valve-assisted cell seeding microfluidic systems that require permanent external pneumatic actuators.<sup>27,28</sup> Another benefit of using the normally-closed valves is to isolate each microchamber from the cell inlet and outlet ports that typically have accumulated many cells ( $>10^6$  cells/ml) that consume much of the nutrients and generate a significant amount of waste products.

As an example of how these microchambers can be configured together, we present an integrated microfluidic device that generates all combinations of overlapping gradient profiles by multiplexing solutions from open reservoirs to discrete cell chambers. The device contains three open solution reservoirs and six microchambers (Fig. 4A, B). As discussed above, each microchamber is flanked by two normally-closed valves and two embedded porous filters, and also has access to a cell inlet and cell outlet. To integrate the microchamber subunits together, the fluidic channels, valves, and cell ports are designed as shown in Fig. 4A and 4B. Three microchambers are connected in series by



**Fig. 1** Composite layers of a single microchamber. (A) 3D schematic view of the orientation by which all layers are brought together. Each layer is made of PDMS except polycarbonate filters and bonded together by plasma oxidation. The membrane layers are 20  $\mu$ m thick and the polycarbonate filters are 10  $\mu$ m thick. (B) 2D schematic view of the top layer, membrane, and bottom layer and the key features for each layer.

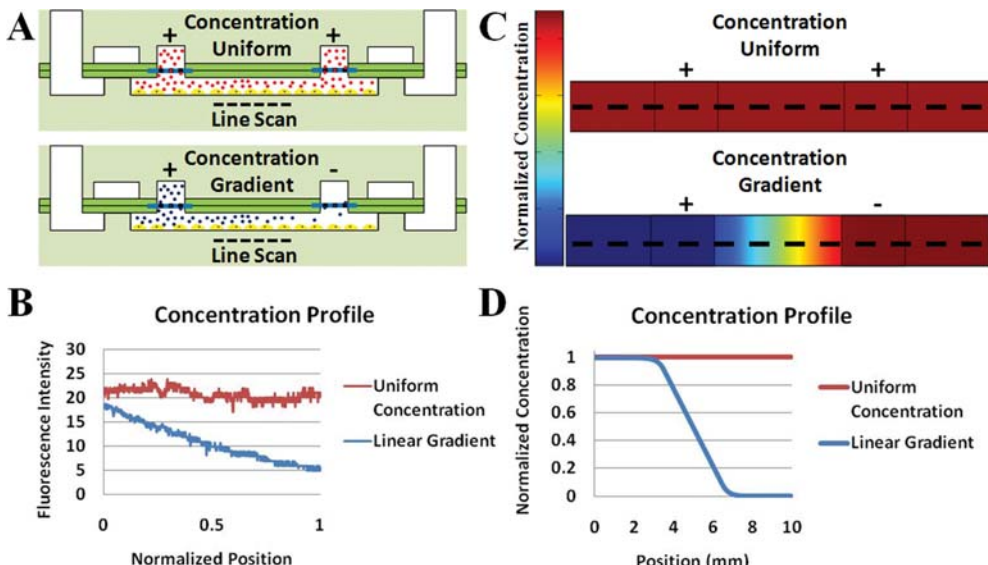


**Fig. 2** Concentration profile in a microchamber. (A) Schematic of diffusing molecules when they exist in both channels (top) or in only one fluid channel (bottom). (B) Fluorescence intensity profile for both scenarios corresponding to line scans in panel A, which yield a uniform concentration profile or linear gradient profile. (C-D) Simulated concentration map and profiles for both cases as in panels A and B.

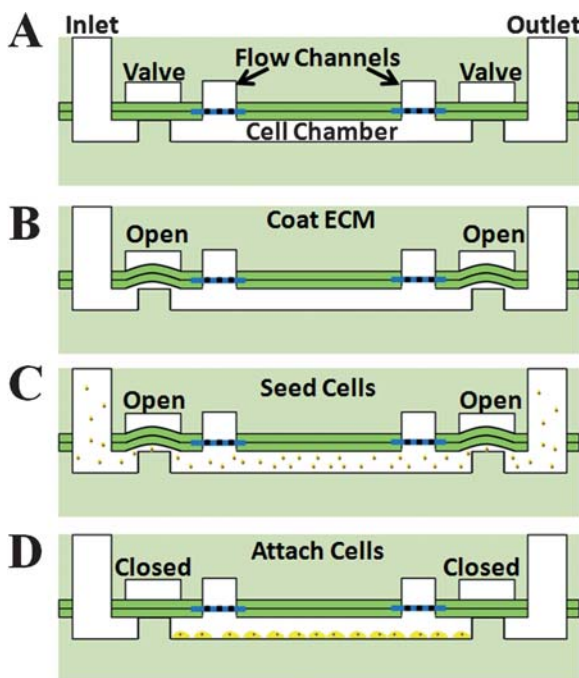


**Fig. 3** Cell Seeding Schematic. (A) Each chamber is isolated by two valves and has two fluidic channels separated by a  $10\ \mu\text{m}$  filter. (B) Valves can be opened to allow flow of ECM protein-containing solutions to render the PDMS surface more biocompatible. (C) Cells subsequently are flowed through to provide a uniform distribution of cells across the channel. (D) Valves are closed to isolate the cell chamber and stop convective flow, which allows cells to settle and attach to the bottom surface of the cell chamber.

sharing one of the flanking valves (*i.e.* 3 microchambers need 4 valves). Microchambers are also integrated in parallel such that fluid channel networks of one microchamber connect to the fluid channel networks of another microchamber. In order to seed all

the chambers from a single cell inlet, all the normally-closed valves are connected to a single vacuum port that simultaneously opens all the valves with a negative pressure induced by a syringe or pipette filler. Alternatively, additional vacuum ports can be added to allow different cell types or ECM coatings to be delivered to only certain microchambers. The channel networks are designed such that each solution (shown as red, green, and yellow in Fig. 4A) is delivered to the six microchambers in different pairings at the two fluid channels above the filters. To accomplish this, the fluidic channels bypass each other by access holes between the top and bottom layer as shown in Fig. 4A. With this configuration, three microchambers have a uniform concentration profile of each food dye solution and another three microchambers have overlapping gradients of each food dye solution (Fig. 4C). Fig. 4D shows a close-up image of an overlapping gradient of red and green food dyes (chamber 5 in Fig. 4C). The normally-closed valves at each end of the microchambers completely segregate the solutions from cross-contamination when in a closed state (Fig. 4E).

To demonstrate the suitability of the device for mammalian cell culture, we used mESCs that are known to be sensitive to their microenvironment.<sup>28,29</sup> Fig. 5A is a phase image of cells three hours after seeding in one of the microchambers. The attached cells are uniformly distributed within the microchamber and well-spread. Fig. 5B is a plot of the average cell density for each of the six microchambers. It can be seen that despite the cell suspension flowing from a single inlet to all six chambers arranged both in parallel and in series, all chambers have similar cell densities. In addition, the relatively small error bars demonstrate that variation between devices is minimal.

In order to show that this device functions for long-term experiments, we performed an experiment that exposed breast cancer cells (MDA-MB-231) to staining solutions for a 24 h period. Fig. 5C shows fluorescent images of the six microchambers with cells fluorescing varying levels of green and red

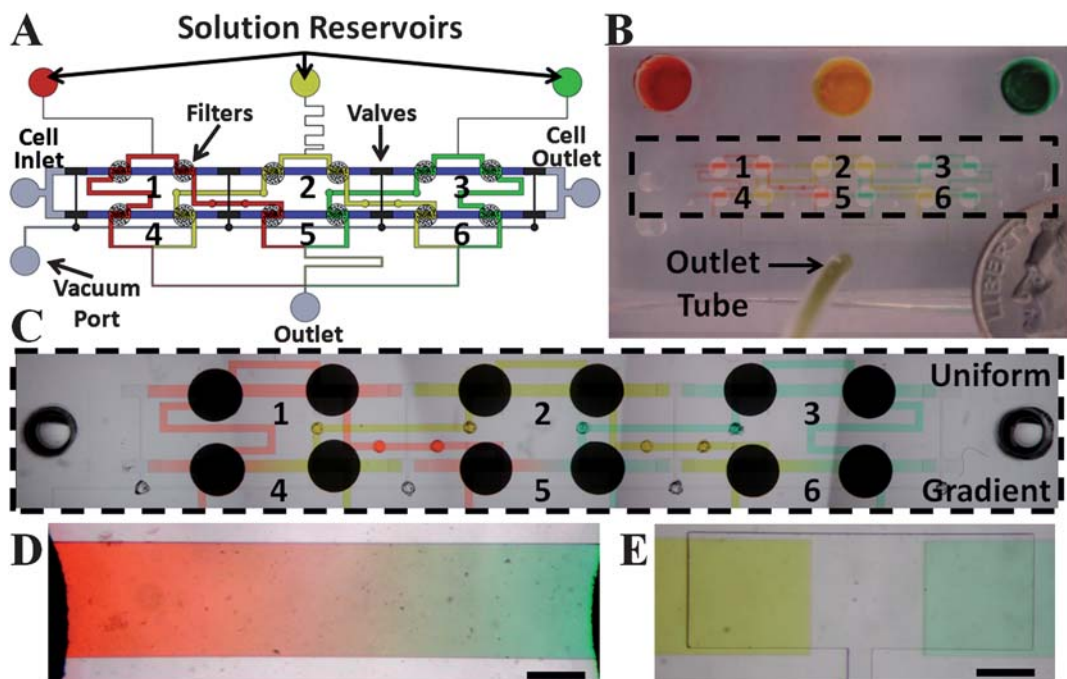


**Fig. 4** Overlapping Static Gradient Device. (A) Schematic of the channel networks designed such that each microchamber has a different combination of the three possible solutions (red, yellow, and green) flowing over its two filters. The cell chambers are shown in blue. (B) Actual image of device with three different color food dyes, corresponding to panel A, to visualize channel networks and gradient in the microchambers. (C) Close-up image of microchambers, top row has a uniform concentration profile in each microchamber and bottom row has an overlapping gradient of two dyes. Black circles are porous filter of 2 mm in diameter. (D) Close-up image of cell chamber number 5 that has an overlapping gradient of red and green dye. Scale Bar: 250  $\mu\text{m}$ . (E) Close-up image of an embedded valve that isolates two microchambers when in a closed position. Scale Bar: 250  $\mu\text{m}$ .

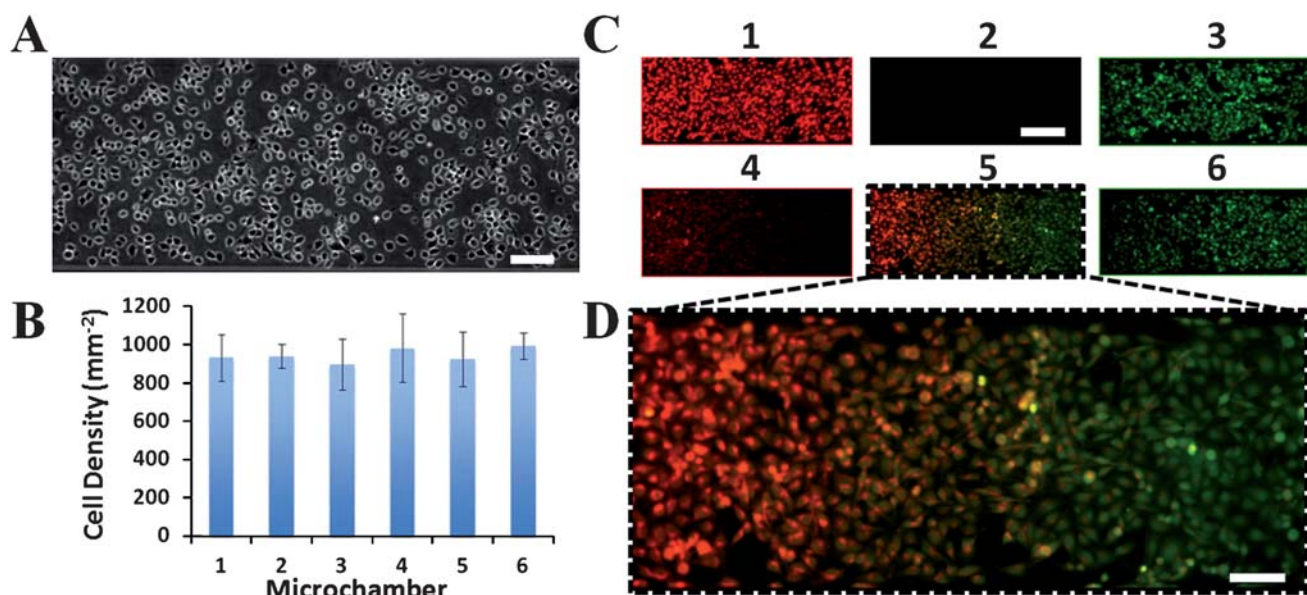


**Fig. 5** Uniform Cell Seeding. (A) Phase image of cells three hours after seeding into the device. Scale Bar: 100  $\mu\text{m}$ . (B) Graph of cell density in each microchamber averaged over three separate devices. (C) Fluorescent images of each microchamber in the device multiplexing a green stain solution, a buffer solution, and a red stain solution. Scale Bar: 250  $\mu\text{m}$ . (D) Close-up fluorescent image of chamber 5 showing an overlapping gradient of green and red stains. Scale Bar: 100  $\mu\text{m}$ .

stains corresponding to the overlapping gradient profiles of each chamber. Fig. 5D shows a close-up image of cell chamber 5 with an overlapping gradient of cell trackers green and red. This test shows the normally-closed valves can be reopened to allow

subsequent washing treatments of the microchambers, which were needed to remove the staining solutions in this case. The capability to reopen and close valves enables dynamic functionality of the device, for example, layer-by-layer coating of

ECM proteins,<sup>30</sup> initial seeding of feeder cells,<sup>29</sup> or providing a periodic spike of a stimulant to cells.<sup>31</sup>

## Conclusion

We presented a microfluidic device that can generate six distinct fluidic conditions in six discrete cell chambers from only three solutions in open reservoirs. The device incorporates normally-closed valves to allow for easy seeding of cells uniformly into each chamber simply by pipetting a single cell suspension into a single inlet port and inducing a gravity-driven flow. The wasting of test solutions is significantly minimized by designing channel networks that equally withdraw solutions from open reservoirs to a single outflow port thereby negating the requirement for dead-volume tubing to infuse the test solutions. The multiplexed chamber format enables several test conditions to be evaluated simultaneously, minimizing variance between experiments. The demonstration of a population of cells taking up stain according to their spatial position in a gradient can be expanded to study downstream cellular processes such as chemotaxis,<sup>3–5</sup> differentiation,<sup>6–8</sup> or drug-sensitivity.<sup>32</sup> Since there is no flow in cell chambers, this platform can be used with non-adherent or sensitive cells such as hematopoietic stem cells,<sup>33</sup> neurons,<sup>34</sup> and cell spheroids.<sup>25</sup> In addition, the device can be designed to have different configurations of the microchambers in order to accommodate additional solution reservoirs and more test conditions on the same chip.

## Acknowledgements

We thank the NIH (HL-084370) for financial support. B.M. acknowledges funding TEAM training grant support from the National Institute for Dental and Craniofacial Research.

## References

- 1 G. Velve-Casquillas, M. Le Berre, M. Piel and P. T. Tran, *Nano Today*, 2010, **5**, 28–47.
- 2 T. M. Keenan and A. Folch, *Lab Chip*, 2008, **8**, 34–57.
- 3 S. J. Wang, W. Saadi, F. Lin, C. M. C. Nguyen and N. L. Jeon, *Exp. Cell Res.*, 2004, **300**, 180–189.
- 4 N. L. Jeon, H. Baskaran, S. K. W. Dertinger, G. M. Whitesides, L. Van de Water and M. Toner, *Nat Biotechnol*, 2002, **20**, 826–830.
- 5 B. Mosadegh, W. Saadi, S. J. Wang and N. L. Jeon, *Biotechnol. Bioeng.*, 2008, **100**, 1205–1213.
- 6 J. Y. Park, S. K. Kim, D. H. Woo, E. J. Lee, J. H. Kim and S. H. Lee, *Stem Cells*, 2009, **27**, 2646–2654.
- 7 B. G. Chung, L. A. Flanagan, S. W. Rhee, P. H. Schwartz, A. P. Lee, E. S. Monuki and N. L. Jeon, *Lab Chip*, 2005, **5**, 401–406.
- 8 W. T. Fung, A. Beyzavi, P. Abgrall, N. T. Nguyen and H. Y. Li, *Lab Chip*, 2009, **9**, 2591–2595.
- 9 A. E. Kamholz, B. H. Weigl, B. A. Finlayson and P. Yager, *Anal. Chem.*, 1999, **71**, 5340–5347.
- 10 S. K. W. Dertinger, D. T. Chiu, N. L. Jeon and G. M. Whitesides, *Anal. Chem.*, 2001, **73**, 1240–1246.
- 11 G. M. Walker, J. Q. Sai, A. Richmond, M. Stremler, C. Y. Chung and J. P. Wikswo, *Lab Chip*, 2005, **5**, 611–618.
- 12 B. Mosadegh, C. Huang, J. W. Park, H. S. Shin, B. G. Chung, S. K. Hwang, K. H. Lee, H. J. Kim, J. Brody and N. L. Jeon, *Langmuir*, 2007, **23**, 10910–10912.
- 13 V. V. Abhyankar, M. A. Lokuta, A. Huttenlocher and D. J. Beebe, *Lab Chip*, 2006, **6**, 389–393.
- 14 C. W. Frevert, G. Boggy, T. M. Keenan and A. Folch, *Lab Chip*, 2006, **6**, 849–856.
- 15 Y. Du, J. Shim, M. Vidula, M. J. Hancock, E. Lo, B. G. Chung, J. T. Borenstein, M. Khabiry, D. M. Cropek and A. Khademhosseini, *Lab Chip*, 2009, **9**, 761–767.
- 16 W. Saadi, S. W. Rhee, F. Lin, B. Vahidi, B. G. Chung and N. L. Jeon, *Biomed. Microdevices*, 2007, **9**, 627–635.
- 17 T. M. Keenan, C. H. Hsu and A. Folch, *Appl. Phys. Lett.*, 2006, **89**, 114103.
- 18 S. Paliwal, P. A. Iglesias, K. Campbell, Z. Hilioti, A. Groisman and A. Levchenko, *Nature*, 2007, **446**, 46–51.
- 19 D. Kim, M. A. Lokuta, A. Huttenlocher and D. J. Beebe, *Lab Chip*, 2009, **9**, 1797–1800.
- 20 T. Kim, M. Pinelis and M. M. Maharbiz, *Biomed. Microdevices*, 2009, **11**, 65–73.
- 21 H. K. Wu, B. Huang and R. N. Zare, *J. Am. Chem. Soc.*, 2006, **128**, 4194–4195.
- 22 S. Y. Cheng, S. Heilman, M. Wasserman, S. Archer, M. L. Shuler and M. M. Wu, *Lab Chip*, 2007, **7**, 763–769.
- 23 B. Mosadegh, C.-H. Kuo, Y.-C. Tung, Y. Torisawa, T. Bersano-Begey and S. Takayama, *Nat. Phys.*, 2010, **6**, 433–437.
- 24 D. C. Duffy, J. C. McDonald, O. J. A. Schueller and G. M. Whitesides, *Anal. Chem.*, 1998, **70**, 4974–4984.
- 25 Y. S. Torisawa, B. Mosadegh, G. D. Luker, M. Morell, K. S. O’Shea and S. Takayama, *Integr. Biol.*, 2009, **1**, 649–654.
- 26 R. D. Lovchik, F. Bianco, M. Matteoli and E. Delamarche, *Lab Chip*, 2009, **9**, 1395–1402.
- 27 Z. H. Wang, M. C. Kim, M. Marquez and T. Thorsen, *Lab Chip*, 2007, **7**, 740–745.
- 28 K. I. Kamei, S. L. Guo, Z. T. F. Yu, H. Takahashi, E. Gschwend, C. Suh, X. P. Wang, J. G. Tang, J. McLaughlin, O. N. Witte, K. B. Lee and H. R. Tseng, *Lab Chip*, 2009, **9**, 555–563.
- 29 H. Tavana, B. Mosadegh and S. Takayama, *Adv. Mater.*, 2010, **22**, 2628–2631.
- 30 G. Mehta, M. J. Kiel, J. W. Lee, N. Kotov, J. J. Linderman and S. Takayama, *Adv. Funct. Mater.*, 2007, **17**, 2701–2709.
- 31 A. Jovic, B. Howell and S. Takayama, *Microfluid. Nanofluid.*, 2009, **6**, 717–729.
- 32 X. Y. Zhu, L. Y. Chu, B. H. Chueh, M. W. Shen, B. Hazarika, N. Phadke and S. Takayama, *Analyst*, 2004, **129**, 1026–1031.
- 33 S. L. Faley, M. Copland, D. Wlodkowic, W. Kolch, K. T. Seale, J. P. Wikswo and J. M. Cooper, *Lab Chip*, 2009, **9**, 2659–2664.
- 34 A. M. Taylor, M. Blurton-Jones, S. W. Rhee, D. H. Cribbs, C. W. Cotman and N. L. Jeon, *Nat. Methods*, 2005, **2**, 599–605.